

APPLICATION OF A 6DOF ALGORITHM FOR THE INVESTIGATION OF IMPULSE WAVES GENERATED DUE TO SUB-AERIAL LANDSLIDES

ARUN KAMATH*, HANS BIHS AND ØIVIND A. ARNTSEN

* DEPARTMENT OF CIVIL AND ENVIRONMENTAL ENGINEERING
NORWEGIAN UNIVERSITY OF SCIENCE AND TECHNOLOGY
NTNU TRONDHEIM, NORWAY
e-mail: arun.kamath@ntnu.no

Key words: Landslide, Tsunami, 6DOF, CFD, REEF3D

Abstract. Inland water bodies such as lakes, rivers and streams are generally considered safe from extreme wave events. Such inland water bodies are susceptible to extreme wave events due to impact of aerial landslides, where a large mass of land impacts the water at high velocities, resulting in a sudden transfer of momentum to the water body. Similar events can occur due to an underwater landslide as well. The evaluation of such extreme events in inland water bodies and the impact of such extreme waves on the regions adjacent to the water body is essential to assess the safety of the constructions on the banks of the water bodies. The generation of extreme waves due to aerial and sub-aerial landslides depends on several parameters such as the height of fall, the composition of the impacting land mass and the bottom slope of the water body.

In this paper, the 6DOF algorithm implemented in the open source Computational Fluid Dynamics (CFD) model REEF3D is used to simulate the motion of a sliding wedge impacting the water free surface. This is used to represent a sliding landmass impacting water after a landslide event. The wedge is represented using a primitive triangular surface mesh and a ray-tracing algorithm is used to determine the position of the object with respect to the underlying grid. Further, the level set method is then used to represent the solid boundary. The motion of the wedge is obtained by propagating the level set equation. The interaction of the wedge with the free water surface is obtained in a sharp and accurate manner using the level set method for both the water free surface and the solid boundary. REEF3D uses a staggered Cartesian numerical grid with a fifth-order WENO scheme for convection discretisation and a third-order Runge-Kutta scheme for time advancement. With the higher-order methods and the level set method, the model can be used to calculate detailed flow information such as the pressure changes in the water on impact and the associated deformation of the water free surface. The accurate representation of these characteristics is essential for correctly evaluating the height and period of the generated extreme wave and associated properties such as the wave celerity and wave run up on the banks during the extreme event.

1 INTRODUCTION

The impact of large landmasses on confined interior water bodies can have disastrous consequences. The generation of tsunamis in the ocean due to natural activities such as earthquakes and volcanic eruptions have been studied from different perspectives, geological and hydrodynamic. On the other hand, the generation of an extreme tsunami-like wave in an inland water body due to landslides presents several interesting problems to investigate, model and obtain more insights. Landslide impact on water results in a sudden transfer of momentum from the falling landmass to water. This displaces a large amount of water while providing it sufficient energy that results in a large tsunami-like wave as the displaced mass of water approaches the shore. The fall event can also result in large run ups at the near shore that is upstream of the fall event. The waves generated by the landslide depends on several factors such as the physical properties of the sliding mass such as its density and volume, in addition to the local topographical features such as the water depth and bottom slope. The height of fall and the composition of the sliding mass also influence the wave generation.

Due to the large number of variables that can influence the tsunami-like wave generation due to a landslide event, numerical modelling of such events can be employed to simulate the different circumstances. With advances in computational power and high performance computing, a numerical model based on the Navier-Stokes equations can be used to calculate the impact of the moving land mass and the influence of this impact on water in a detailed manner.

In this study, the open-source CFD model REEF3D [1], developed at the Department of Civil and Environmental Engineering, NTNU Trondheim is used to simulate the impact of a slide with water. The model has been previously applied to study several marine engineering problems such as breaking wave kinematics [2], calculation of wave forces [3] [4] and floating bodies in waves [5]. In this paper, the 6DOF algorithm in REEF3D is used to model the motion of a wedge driven down a slide to simulate a sub-aerial landslide. The impact of the wedge with water and the calculated resulting free surface features are presented. The numerical results are compared to experimental data for the free surface elevations at various locations in the tank around the region of impact of the wedge.

2 NUMERICAL MODEL

The incompressible Reynolds-averaged Navier-Stokes (RANS) equations are the governing equations of the numerical model.

$$\frac{\partial u_i}{\partial x_i} = 0 \quad (1)$$

$$\frac{\partial u_i}{\partial t} + u_j \frac{\partial u_i}{\partial x_j} = -\frac{1}{\rho} \frac{\partial p}{\partial x_i} + \frac{\partial}{\partial x_j} \left[\left(\frac{\partial u_i}{\partial x_j} + \frac{\partial u_j}{\partial x_i} \right) \right] + g_i \quad (2)$$

where u is the velocity averaged over time t , ρ is the fluid density, p is the pressure, ν is the kinematic viscosity and g the gravity term. The convective terms of the RANS equations are discretized with the fifth-order WENO scheme by Jiang and Shu [6] in the conservative finite-difference framework. The Jacobi-Hamilton version of the WENO scheme [7] is used for the variables of the free surface algorithm. Time integration is carried out using a 2nd-order

TVD Runge-Kutta scheme [8]. The numerical model is based on a Staggered Cartesian grid making the implementation of higher order schemes easier and providing good pressure-velocity coupling. The CFL number is used to govern the time steps in the simulation with an adaptive time stepping method. This maintains the required time step for the stability of the simulation while being economical on the computational cost of the simulation.

Chorin's projection method [9] method is used for pressure treatment and the resulting Poisson pressure equation is solved using the geometric multigrid PFMG preconditioned [10] BiCGStab solver [11] available through the high performance solver library HYPRE [12]. The level set method [13] is used to obtain the free surface and the level set function is reinitialized every time step using the PDE based method [14] to maintain its signed distance property.

The 6DOF algorithm is used to simulate the motion of the wedge. The geometry of the wedge is defined by a primitive triangular surface mesh resembling the STL format used as a standard in design and meshing software. The ray tracing algorithm [15] is used to determine the intersection of the underlying Cartesian grid with the surface mesh. Then, signed distance property of the level set function in the vicinity of the body is obtained with the standard reinitialization algorithm [16]. The ray-tracing algorithm provides a sharp representation of the solid-fluid interface with exact calculation of the distances close the solid boundary. The moving solid-fluid interface is treated with the ghost cell immersed boundary method [17]. Further details about the 6DOF algorithm and its implementation in REEF3D can be found in Bihs et al. [5].

3 RESULTS AND DISCUSSION

3.1 Disc entry

The 6DOF algorithm in REEF3D is validated for the popular disc entry problem, where a solid disc enters water under controlled fall. This case has been presented by several authors such as [18] and [19] as benchmark tests for their models. The non-dimensional parameters for the geometry, the initial boundary conditions and flow parameters for this case are as follows. The disc impacts the water surface travelling under a fixed vertical velocity of $V = -1$. The center of the disc with radius $R = 1$ is located at $H = 1.25$ over the free surface at $t' = Vt/H = 0$. The two-dimensional simulation domain is $30R \times 22R$ long and high respectively and carried out with a uniform mesh of $dx = 0.025$. The simulation is carried out with 1200×880 grid cells. The acceleration due to gravity is $g = 1$, the density of the water $\rho_{water} = 1$, the density of the air $\rho_{air} = 0.001$, the viscosity of the water $\nu_{water} = 0.001$ and the viscosity of the air $\nu_{air} = 0.018$. The time step size is controlled with adaptive time stepping using a CFL number of 0.1.

The free surface location and contour for the velocity magnitude are shown in Fig. 1. The disc enters the water mass in Fig. 1a. Breaking waves are generated in a symmetric fashion, when the disc impacts the free surface. In general terms, the representation of the formation of these breaking waves needs a sufficiently fine mesh [20] and specifically in the current case [19]. In Fig. 1b, the post-breaking waves are seen moving away towards the side walls as the disc is further immersed into water. At $t' = 3.0$, the parted free surface reconnects over the upper surface of the disc as it is completely immersed in water in Fig. (1c). At $t' = 4.0$, the water mass that reconnected over the disc creates a vertical water jet after the impact of the disc. The free

surface location compares well with other results reported in literature.

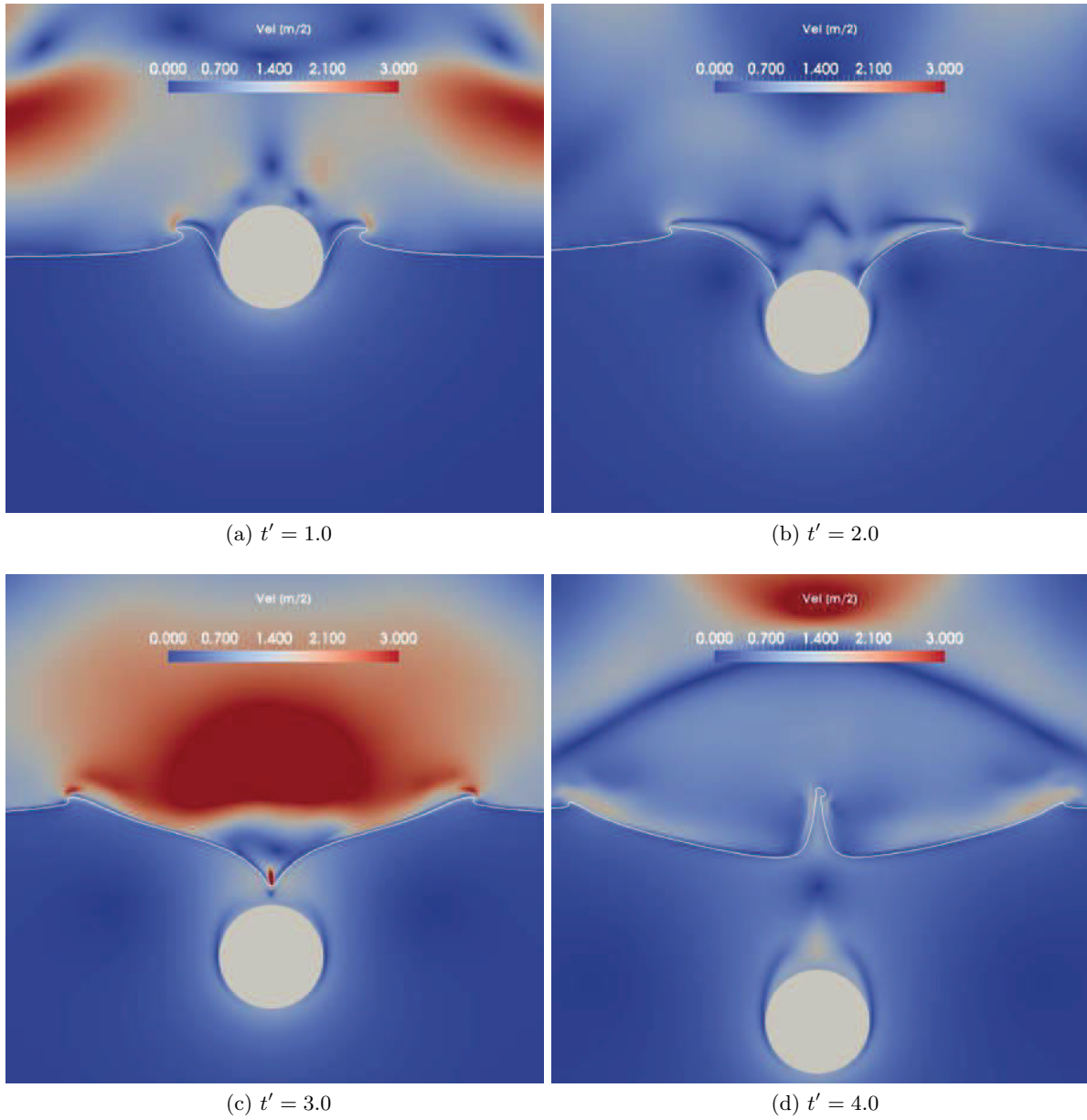


Figure 1: Controlled fall of disc into water showing velocity magnitude contours

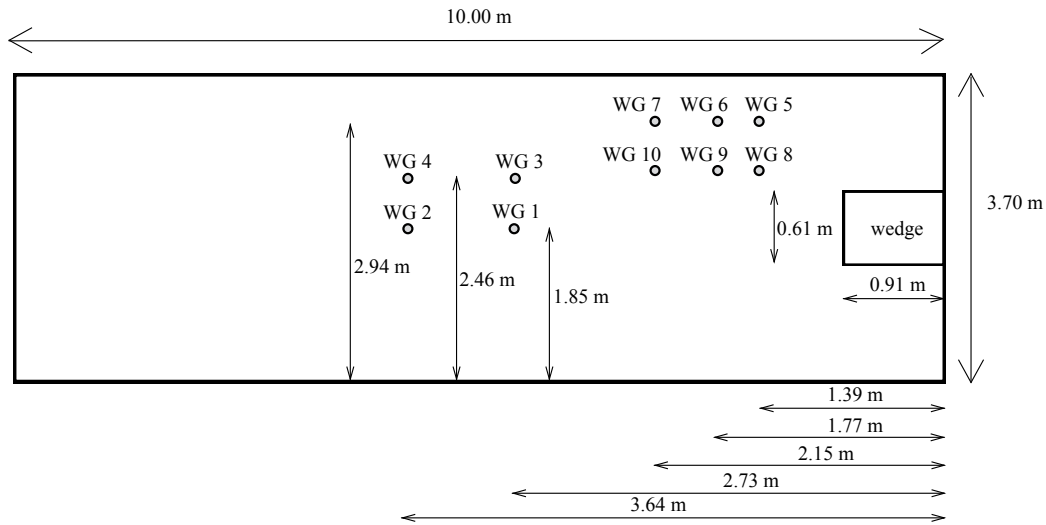
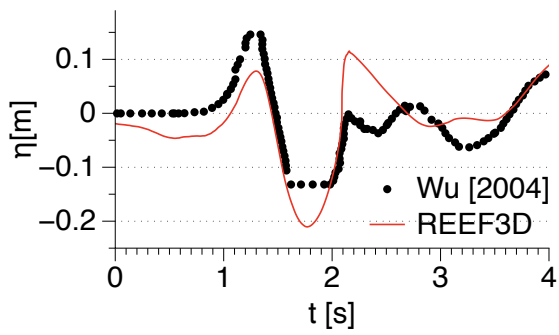


Figure 2: Plan view of the the numerical flume setup used for simulation of the impact of a sliding mass on water

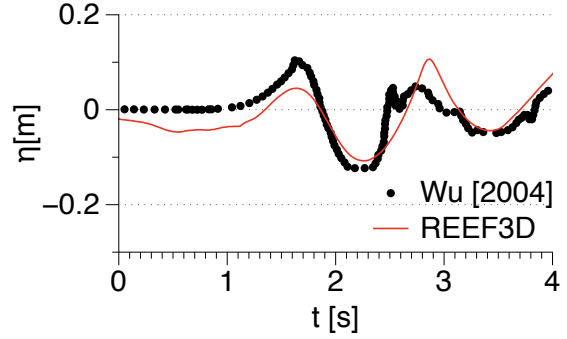
3.2 Impact of a sliding wedge on water

The impact of a sliding wedge into a body of water is simulated in this section. The experimental results presented by [21] are used to compare the numerical results for the free surface elevation. The wedge has a width of 0.61 m and a height of 0.46 m and a length of 0.91 m. The wedge is placed such that the top of the wedge is 0.454 m above the still water level. The wedge is then allowed to slide into water in a controlled manner. The numerical setup is presented in Fig. (2). Wave gages are placed at various locations in the numerical flume to measure the free surface elevation due to the tsunami-like wave caused by the impact of the wedge. A grid size of $dx = 0.05$ m is used in the simulation.

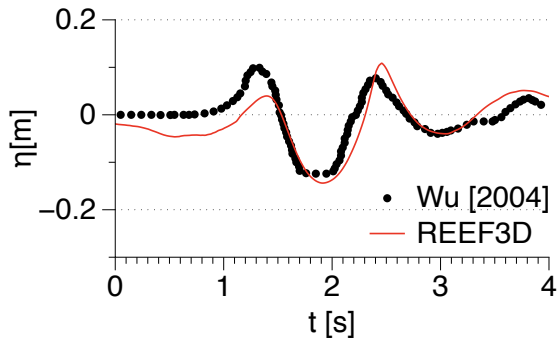
The calculated free surface elevations at the different wave gages placed in the numerical flume are compared with the experimental data in Fig. (3). The numerical results show a reasonable agreement with the experimental observations. At WG 1, the first wave is slightly underestimated while the following wave is overestimated in Fig. (3a). This observed difference is reduced at WG 2 placed a little in front of WG 1 as seen in Fig. (3b). The numerically calculated free surface elevation at wave gages WG 3 and WG 4, placed along the line $y = 2.46$ m are seen to show a good agreement with the experimental data in Figs. (3c) and (3d). The free surface elevations calculated at wave gages WG 5, WG 6, WG 7 and WG 8 in Figs. (3e), (3f), (3g) and (3h) respectively underestimate the free surface elevation in the first 1 s of the simulation as the wedge impacts the water surface but the agreement between the numerical and experimental results improves afterwards. The wave gages WG 9 and WG 10 also underestimate the first wave while the second wave is represented correctly as seen in Figs. (3i) and (3j).



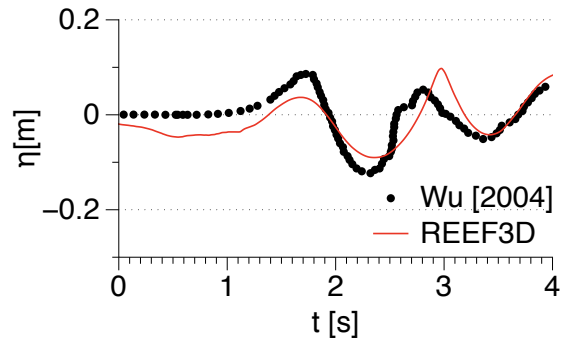
(a) WG 1 at $x = 2.73$ m, $y = 1.85$ m



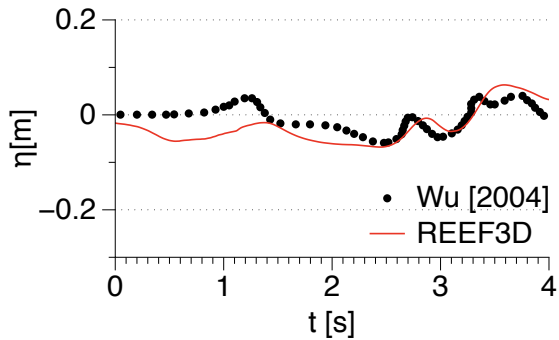
(b) WG 2 at $x = 3.64$ m, $y = 1.85$ m



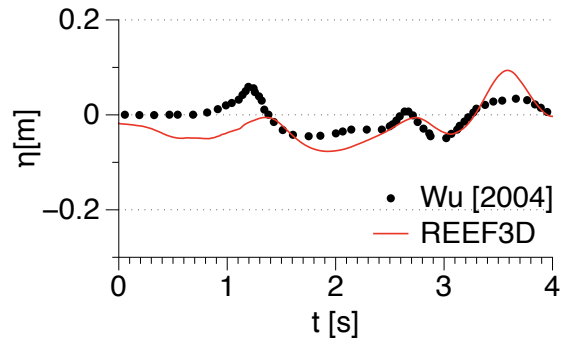
(c) WG 3 at $x = 2.73$ m, $y = 2.46$ m



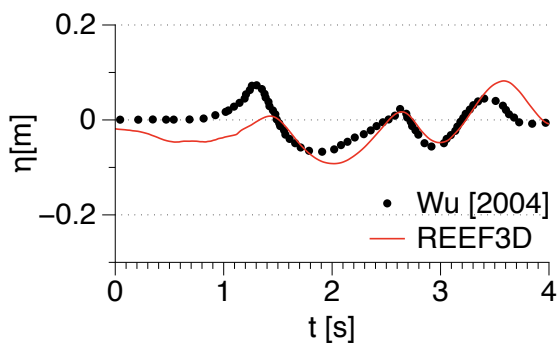
(d) WG 4 at $x = 3.64$ m, $y = 2.46$ m



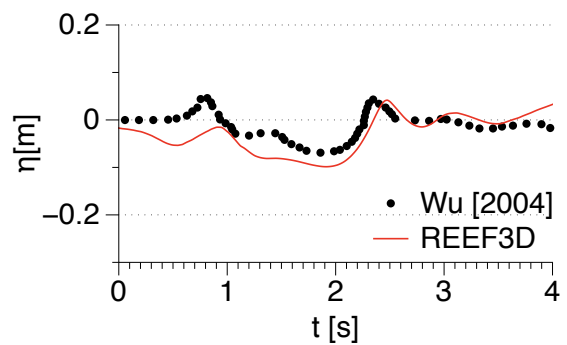
(e) WG 5 at $x = 1.39$ m, $y = 2.94$ m



(f) WG 6 at $x = 1.77$ m, $y = 2.94$ m

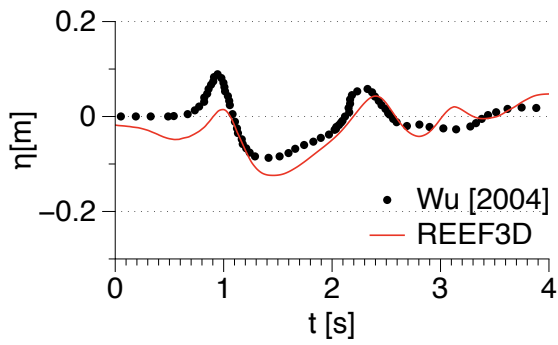


(g) WG 7 at $x = 2.15$ m, $y = 2.94$ m

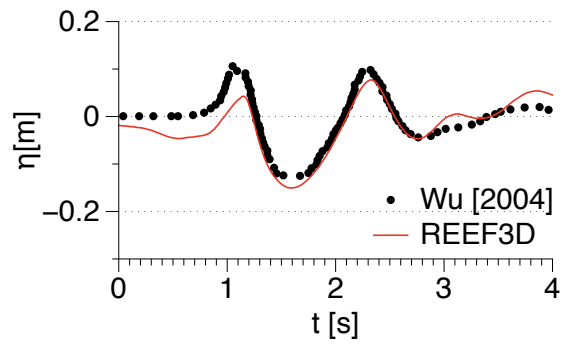


(h) WG 8 at $x = 1.39$ m, $y = 2.46$ m

6

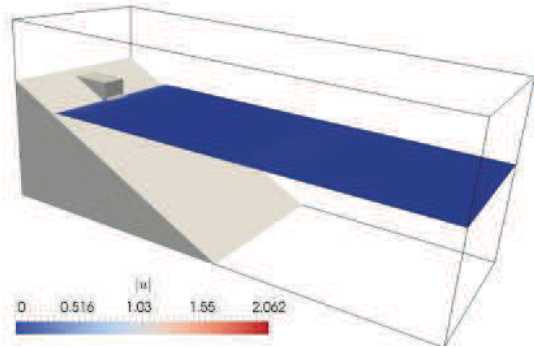


(i) WG 9 at $x = 1.77$ m, $y = 2.46$ m

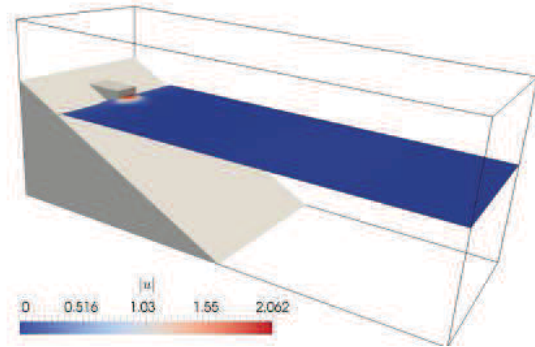


(j) WG 10 at $x = 2.15$ m, $y = 2.46$ m

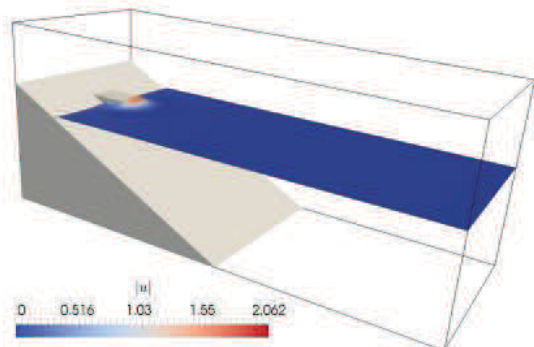
Figure 3: Comparison of the numerical results to the experimental data for the free surface elevation in the wave tank due to the sliding mass impact with water



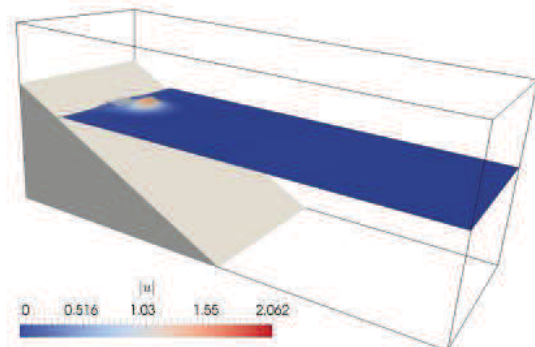
(a) $t = 0.40$ s



(b) $t = 0.60$ s



(c) $t = 0.75$ s



(d) $t = 0.88$ s

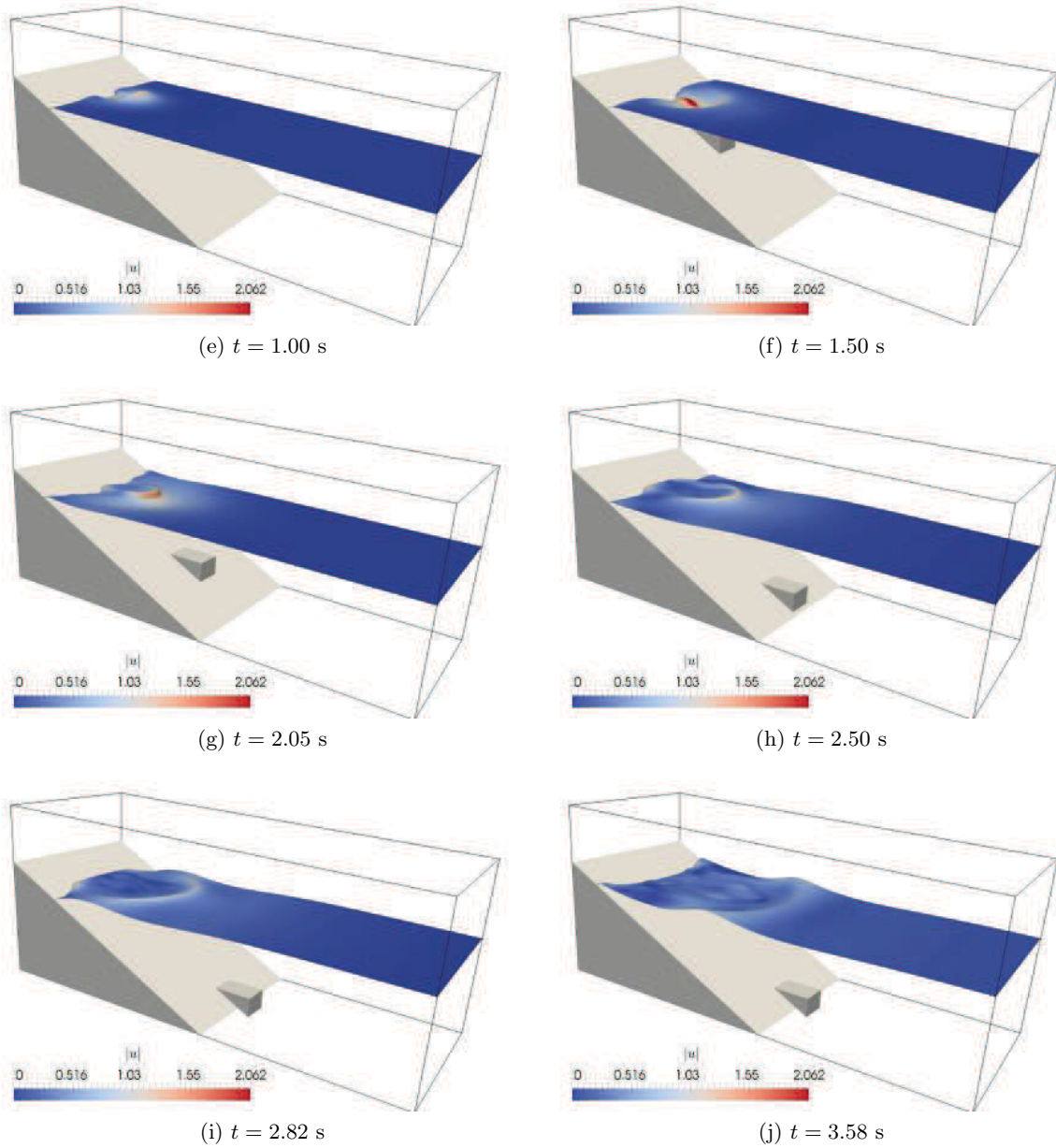


Figure 4: Calculated evolution of the free surface in the numerical flume due to impact of the wedge showing velocity magnitude contours

The evolution of the free surface due to the impact of the wedge is presented in Fig. (4). The impact of the wedge with the free water surface is just initiated at $t = 0.40$ s in Fig. (4a). Half the front surface of the wedge is immersed in water after $t = 0.60$ s in Fig. (4b). The top of the wedge is seen to be at the same level as the initial free surface at $t = 0.75$ s in Fig. (4c). The wedge is just completely immersed in water at $t = 0.88$ s as seen in Fig. (4d). The generation of the water jet due to the immersion of the wedge in to the water body is seen in Figs. (4e), (4f), (4g) and (4h). The propagation of the extreme wave after the wedge has reached the bottom of the slope is seen in Figs. (4i) and (4j).

4 CONCLUSIONS

- The numerical model REEF3D is used to simulate the controlled motion of a wedge in to water and the numerical results show a reasonable agreement with experimental data.
- Future studies on refined grids and for submerged slides will be carried out.

REFERENCES

- [1] Bihs, H., Kamath, A., Alagan Chella, M., Aggarwal, A. and Arntsen, Ø.A. A new level set numerical wave tank with improved density interpolation for complex wave hydrodynamics. *Computers & Fluids* 2016. **140**:191–208.
- [2] Alagan Chella, M., Bihs, H. and Myrhaug, D. Characteristics and profile asymmetry properties of waves breaking over an impermeable submerged reef. *Coastal Engineering* 2015. **100**:26–36.
- [3] Kamath, A., Alagan Chella, M., Bihs, H. and Arntsen, Ø.A. Cfd investigations of wave interaction with a pair of large tandem cylinders. *Ocean Engineering* 2015. **108**:738–748.
- [4] Kamath, A., Alagan Chella, M., Bihs, H. and Arntsen, Ø.A. Breaking wave interaction with a vertical cylinder and the effect of breaker location. *Ocean Engineering* 2016. **128**:105–115.
- [5] Bihs, H. and Kamath, A. A combined level set/ghost cell immersed boundary representation for floating body simulations. *International Journal for Numerical Methods in Fluids* 2016:DOI: 10.1002/fld.4333. doi:10.1002/fld.4333.
- [6] Jiang, G.S. and Shu, C.W. Efficient implementation of weighted ENO schemes. *Journal of Computational Physics* 1996. **126**:202–228.
- [7] Jiang, G.S. and Peng, D. Weighted ENO schemes for Hamilton-Jacobi equations. *SIAM Journal on Scientific Computing* 2000. **21**:2126–2143.
- [8] Shu, C. and Gottlieb, S. Total variation diminishing Runge- Kutta schemes. *Mathematics of Computation* 1998. **67**:73–85.
- [9] Chorin, A. Numerical solution of the Navier-Stokes equations. *Mathematics of Computation* 1968. **22**:745–762.

- [10] Ashby, S.F. and Flagout, R.D. A parallel multigrid preconditioned conjugate gradient algorithm for groundwater flow simulations. *Nuclear Science and Engineering* 1996. **124**(1):145–159.
- [11] van der Vorst, H. BiCGStab: A fast and smoothly converging variant of Bi-CG for the solution of nonsymmetric linear systems. *SIAM Journal on Scientific and Statistical Computing* 1992. **13**:631–644.
- [12] Center for Applied Scientific Computing, Lawrence Livermore National Laboratory. *HYPRE high performance preconditioners - User's Manual*, 2015.
- [13] Osher, S. and Sethian, J.A. Fronts propagating with curvature- dependent speed: algorithms based on Hamilton-Jacobi formulations. *Journal of Computational Physics* 1988. **79**:12–49.
- [14] Sussman, M., Smereka, P. and Osher, S. A level set approach for computing solutions to incompressible two-phase flow. *Journal of Computational Physics* 1994. **114**:146–159.
- [15] Yang, J. and Stern, F. Robust and efficient setup procedure for complex triangulations in immersed boundary simulations. *Journal of Fluids Engineering* 2013. **135**(10):101107.
- [16] Peng, D., Merriman, B., Osher, S., Zhao, H. and Kang, M. A PDE-based fast local level set method. *Journal of Computational Physics* 1999. **155**:410–438.
- [17] Berthelsen, P.A. and Faltinsen, O.M. A local directional ghost cell approach for incompressible viscous flow problems with irregular boundaries. *Journal of Computational Physics* 2008. **227**:4354–4397.
- [18] Yang, J. and Stern, F. Sharp interface immersed-boundary/level-set method for wave–body interactions. *Journal of Computational Physics* 2009. **228**(17):6590–6616.
- [19] Calderer, A., Kang, S. and Sotiropoulos, F. Level set immersed boundary method for coupled simulation of air/water interaction with complex floating structures. *Journal of Computational Physics* 2014. **277**:201–227.
- [20] Alagan Chella, M., Bihs, H., Myrhaug, D. and Muskulus, M. Breaking characteristics and geometric properties of spilling breakers over slopes. *Coastal Engineering* 2015. **95**:4–19.
- [21] Wu, T.R. *A numerical study of three-dimensional breaking waves and turbulence effects*. Ph.D. thesis, Cornell University, 2004.